Journal of Computational and Applied Mathematics 275 (2015) 139–147

Contents lists available at ScienceDirect

Journal of Computational and Applied Mathematics

journal homepage: www.elsevier.com/locate/cam

A two-grid decoupling method for the mixed Stokes–Darcy model[☆]

Liyun Zuo [a], Yanren Hou [a,b,*]

[a] School of Mathematics and Statistics, Xi'an Jiaotong University, Xi'an, Shaanxi 710049, China

[b] Center for Computational Geosciences, Xi'an Jiaotong University, Xi'an, Shaanxi 710049, China

ARTICLE INFO

Article history:
Received 19 January 2014
Received in revised form 19 June 2014

Keywords:
Stokes equations
Darcy's law
Decoupling
Two-grid algorithm

ABSTRACT

In this paper, we consider the mixed Stokes–Darcy problem which describes a fluid flow coupled with a porous media. We present a modified two-grid method for decoupling this mixed model. Stability is proved and optimal error estimates are derived. The numerical results show that the modified two-grid method is effective and has the same accuracy as the coupling scheme when we choose $h = H^2$.

1. Introduction

Multi-modeling problems have received a wide publicity over the past years due to their applications. We mainly have interest in the mixed Stokes–Darcy model, which describes the coupling of the fluid flow (governed by the Stokes equations) with the porous media flow (governed by the Darcy equations) through certain interface conditions.

Generally speaking, solving this coupled model usually results in difficulties, especially in the numerical implementation. We are interested in the decoupling methods, in which the coupled problems can be separated into two single flow subproblems. This allows us to use suitable methods flexibly for solving each subproblem separately, and numerical implementation is easy and efficient.

Some decoupling technologies have been developed during the last decades. For example, the domain decomposition methods for various coupled models were studied in [1–12], the Lagrange multiplier approach is used in [13,14], the interface relaxation approach is applied in [15,16], precondition techniques are considered in [17,18], and the decoupling marching algorithm based on interface approximation via temporal extrapolation is proposed in [19–22] for same time step length in both subproblems or different time step lengths in different subproblems. In addition, the two-grid method is applied successfully to solve multi-modeling problems in [23–25], using this method, one can get two independent subproblems on certain fine grid since the transmission conditions on the interface can be approximated by the coarse grid approximation. Furthermore, a multilevel decoupled method for the mixed Stokes–Darcy model is proposed in [26]. However, such two-grid and multilevel schemes have not theoretically achieved the optimal error estimates about the L^2-norm of ∇u and p since the interface condition is approximated by the coarse grid approximation. In this paper, we will follow the idea in [25] and propose a modified two-grid method for the mixed Stokes–Darcy model with the Beavers–Joseph–Saffman interface condition. The optimal error estimates are obtained for this method.

☆ Subsidized by NSFC (Grant No. 11171269) and the Ph.D. Programs Foundation of Ministry of Education of China (Grant No. 20110201110027).
* Corresponding author at: School of Mathematics and Statistics, Xi'an Jiaotong University, Xi'an, Shaanxi 710049, China. Tel.: +86 2982663565.
E-mail addresses: xiaoyezi@stu.xjtu.edu.cn (L. Zuo), yrhou@mail.xjtu.edu.cn (Y. Hou).

http://dx.doi.org/10.1016/j.cam.2014.08.008
0377-0427/

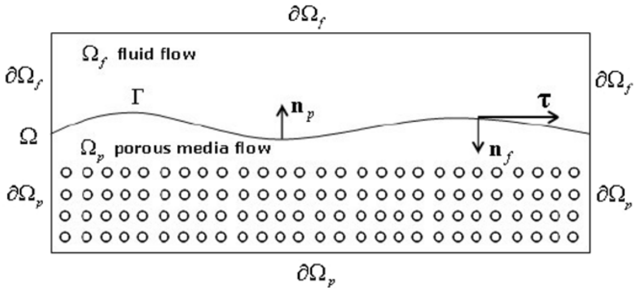

Fig. 1. A global domain Ω consisting of a fluid region Ω_f and a porous region Ω_p separated by an interface Γ.

The rest of the paper is organized as follows. A mixed Stokes–Darcy model is described in the next section. In Section 3, the modified two-grid algorithm is given. Stability is proved and convergence is deduced in Section 4 followed by some numerical experiments in Section 5. Finally, we end this paper with a conclusion in Section 6.

2. Model problem

We consider the model in a bounded domain $\Omega \subset R^d$ ($d = 2$ or 3), which consists of a fluid flow region Ω_f and a porous media region Ω_p, see Fig. 1. Here $\Omega_f \cap \Omega_p = \emptyset$, $\overline{\Omega}_f \cup \overline{\Omega}_p = \overline{\Omega}$. Two domains are separated by the interface $\Gamma = \partial\Omega_f \cap \partial\Omega_p$. Let $\Gamma_f = \partial\Omega_f \setminus \Gamma,\ \Gamma_p = \partial\Omega_p \setminus \Gamma$,

The Stokes equations govern the fluid flow in Ω_f:

$$-\nu\Delta u + \nabla p = f_1 \quad \text{in } \Omega_f, \tag{2.1}$$

$$\nabla \cdot u = 0 \quad \text{in } \Omega_f. \tag{2.2}$$

Here, u and p are the velocity field and the kinetic pressure, ν is the kinetic viscosity, f_1 is the external force.

The Darcy equations govern the porous media flow in Ω_p:

$$u_p = -\mathbf{K}\nabla\varphi \quad \text{in } \Omega_p, \tag{2.3}$$

$$\nabla \cdot u_p = f_2 \quad \text{in } \Omega_p. \tag{2.4}$$

Here u_p and φ are the Darcy velocity and the piezometric head, $\mathbf{K} = \{K_{ij}\}_{d\times d}$ is hydraulic conductivity tensor, denoting permeability of the rock. In this paper, we assume $\mathbf{K}$ is a symmetric and positive definite matrix with the smallest eigenvalue $k_{\min} > 0$. f_2 is the source term satisfying the solvability condition

$$\int_{\Omega_p} f_2 = 0.$$

Combining Darcy's law (2.3) with the continuity equation (2.4), we get the following elliptic equation:

$$-\nabla \cdot (\mathbf{K}\nabla\varphi) = f_2 \quad \text{in } \Omega_p. \tag{2.5}$$

On the interface Γ, we impose the following three interface conditions:

$$u \cdot n_f + u_p \cdot n_p = 0 \quad \text{on } \Gamma, \tag{2.6}$$

$$p - \nu n_f \frac{\partial u}{\partial n_f} = g\varphi \quad \text{on } \Gamma, \tag{2.7}$$

$$-\nu\tau_i \frac{\partial u}{\partial n_f} = \alpha\sqrt{\frac{\nu g}{\mathrm{tr}(\mathbf{K})}}\, u \cdot \tau_i \quad 1 \le i \le (d-1),\ \text{on } \Gamma, \tag{2.8}$$

where, n_f and n_p denote the unit outward normal vectors on $\partial\Omega_f$ and $\partial\Omega_p$, in particularly, $n_p = -n_f$ on the interface Γ. g is the gravitational acceleration, α is a positive parameter depending on the properties of the porous medium, $\tau_i,\ i = 1, \ldots, d-1$, are the unit tangential vectors on the interface Γ. (2.8) is referred to as the Beavers–Joseph–Saffman interface condition, which is the simplified Beavers–Joseph interface condition.

For simplicity, we assume homogeneous Dirichlet boundary conditions are satisfied on Γ_f and Γ_p:

$$u = 0 \quad \text{on } \Gamma_f, \tag{2.9}$$

$$\varphi = 0 \quad \text{on } \Gamma_p. \tag{2.10}$$

The exact boundary conditions chosen above are not essential to either the analysis or the algorithms studied herein.

For $D = \Omega_f$ or Ω_p, let us denote by $(\cdot,\cdot)_D$ the usual L^2-scalar product in $L^2(D)$, and $\|\cdot\|_{L^2(D)}$ the corresponding norm. Define the following spaces:

$$H_f = \{v \in (H^1(\Omega_f))^d : v = 0 \text{ on } \Gamma_f\},$$
$$H_p = \{\psi \in H^1(\Omega_p) : \psi = 0 \text{ on } \Gamma_p\},$$
$$W = H_f \times H_p,$$
$$Q = L^2(\Omega_f).$$

And the space W is equipped with the following norms: $\forall\, w \in W$,

$$\|w\|_0 = \sqrt{(u,u)_{\Omega_f} + (\varphi,\varphi)_{\Omega_p}},$$
$$\|w\|_W = \sqrt{(\nabla u,\nabla u)_{\Omega_f} + (\nabla\varphi,\nabla\varphi)_{\Omega_p}}.$$

We shall assume that g, ν and K are constants, and f_1 and f_2 are smooth enough. Then the weak formulation of the above Stokes–Darcy model reads as follows: find $w = (u,\varphi) \in W$ and $p \in Q$, such that

$$a(w,z) + b(z,p) = f(z) \quad \forall z = (v,\psi) \in W, \tag{2.11}$$
$$b(w,q) = 0 \quad \forall q \in Q, \tag{2.12}$$

where

$$a(w,z) = a_f(u,v) + a_p(\varphi,\psi) + a_\Gamma(w,z),$$
$$a_f(u,v) = \nu(\nabla u,\nabla v)_{\Omega_f} + \alpha\sqrt{\frac{\nu g}{\mathrm{tr}(\mathbf{K})}}\sum_{i=1}^{d-1}\int_\Gamma (u\cdot\tau_i)(v\cdot\tau_i)ds,$$
$$a_p(\varphi,\psi) = g(\mathbf{K}\nabla\varphi,\nabla\psi)_{\Omega_p},$$
$$a_\Gamma(w,z) = g\int_\Gamma (\varphi v\cdot n_f - \psi u\cdot n_f)ds,$$
$$b(z,p) = -(p,\nabla\cdot v)_{\Omega_f},$$
$$f(z) = (f_1,v)_{\Omega_f} + g(f_2,\psi)_{\Omega_p}.$$

In [5,6], the well-posedness of the mixed Stokes–Darcy model (2.11)–(2.12) can be found.

Moreover, for the needs of theoretical analysis, we shall recall the following Poincaré and trace inequalities: there exist constant C_p, C_t that only depend on the domain Ω_f, and $\widetilde{C}_p$, $\widetilde{C}_t$ that only depend on the domain Ω_p, such that for all $v \in H_f$ and $\psi \in H_p$,

$$\|v\|_{L^2(\Omega_f)} \le C_p\|\nabla v\|_{L^2(\Omega_f)}, \qquad \|v\|_{L^2(\Gamma)} \le C_t\|\nabla v\|_{L^2(\Omega_f)}, \tag{2.13}$$
$$\|\psi\|_{L^2(\Omega_p)} \le \widetilde{C}_p\|\nabla\psi\|_{L^2(\Omega_p)}, \qquad \|\psi\|_{L^2(\Gamma)} \le \widetilde{C}_t\|\nabla\psi\|_{L^2(\Omega_p)}. \tag{2.14}$$

3. Numerical algorithms

Let H be a positive parameter tending to 0, τ_H be a quasi-uniform triangulation of the domain $\overline{\Omega}$ into triangles or quadrilaterals with diameters bounded by H. No mesh compatibility or interdomain continuity at the interface is assumed. Let $W_H = H_{fH} \times H_{pH} \subset W$ and $Q_H \subset Q$ be the finite element subspaces defined on the partition τ_H. For another positive parameter h ($h < H$), we introduce another quasi-uniform triangulation τ_h accordingly. And let $W_h = H_{fh} \times H_{ph} \subset W$ and $Q_h \subset Q$ denote the corresponding finite element subspaces. For simplicity, we assume that the two triangulations are nested, i.e., $(W_H, Q_H) \subset (W_h, Q_h) \subset (W, Q)$. Furthermore, we assume that the finite element space pair $(H_{f\tilde{h}}, Q_{\tilde{h}})$, $\tilde{h} = H, h$, satisfies the discrete inf–sup condition: there exists a positive constant β, independent of $\tilde{h}$, such that $\forall\, q_{\tilde{h}} \in Q_{\tilde{h}}$, $\exists\, z_{\tilde{h}} = (v_{\tilde{h}}, 0) \in W_{\tilde{h}}$,

$$b(z_{\tilde{h}}, q_{\tilde{h}}) \ge \beta\|z_{\tilde{h}}\|_W\|q_{\tilde{h}}\|_Q. \tag{3.1}$$

Then the finite element scheme for (2.11)–(2.12) based on (W_h, Q_h) reads:

Algorithm 1 (*Coupling Scheme*)**.** Find $w_h = (u_h,\varphi_h) \in W_h$ and $p_h \in Q_h$ such that

$$a(w_h,z_h) + b(z_h,p_h) = f(z_h) \quad \forall z_h = (v_h,\psi_h) \in W_h, \tag{3.2}$$
$$b(w_h,q_h) = 0 \quad \forall q_h \in Q_h. \tag{3.3}$$

For the system (3.2)–(3.3), one has to solve a coupled problem, which usually results in difficulties in numerical implementation. In [25], Mu and Xu proposed a two-grid scheme for the mixed Stokes–Darcy problem. Then this coupled system can be decoupled into two subproblems by a coarse grid approximation to the interface coupling conditions.

Two-grid approach is efficient and effective for solving multi-modeling problems, such as the mixed Stokes–Darcy problem. The convergence $O(H^{\frac{3}{2}})$ for the fluid velocity and pressure was proved in [25]. However, in [26] numerical experiments showed the convergence rate $O(H^2)$, which implies that the convergence rate for the fluid velocity and pressure may be improved from $O(H^{\frac{3}{2}})$ to $O(H^2)$. Following the idea of [25], we propose a modified two-grid algorithm by a fine grid approximation instead of a coarse grid one to the interface coupling conditions in the Stokes problem.

Algorithm 2 (*Modified Two-Grid Scheme*)**.** Step 1. Solve the coupled problem on a coarse grid: find $w_H = (u_H, \varphi_H) \in W_H$ and $p_H \in Q_H$ such that

$$a(w_H, z_H) + b(z_H, p_H) = f(z_H) \quad \forall z_H = (v_H, \psi_H) \in W_H, \tag{3.4}$$

$$b(w_H, q_H) = 0 \quad \forall q_H \in Q_H. \tag{3.5}$$

Step 2. On the fine grid, we first solve the Darcy problem in Ω_p: find $\overline{\varphi}^h \in H_{ph}$ such that

$$a_p(\overline{\varphi}^h, \psi_h) = g(f_2, \psi_h)_{\Omega_p} + g\int_\Gamma \psi_h u_H \cdot n_f ds, \quad \forall \psi_h \in H_{ph}. \tag{3.6}$$

Then solve the Stokes problem in Ω_f: find $\overline{u}^h \in H_{fh}$ and $\overline{p}^h \in Q_h$ such that

$$a_f(\overline{u}^h, v_h) + b_f(v_h, \overline{p}^h) = (f_1, v_h)_{\Omega_f} - g\int_\Gamma \overline{\varphi}^h v_h \cdot n_f ds \quad \forall v_h \in H_{fh}, \tag{3.7}$$

$$b_f(\overline{u}^h, q_h) = 0 \quad \forall q_h \in Q_h, \tag{3.8}$$

where $b_f(\overline{u}^h, q_h) = -(\nabla \cdot \overline{u}^h, q_h)_{\Omega_f}$.

By this modification, we shall prove that the optimal convergence order of ∇u and p in L^2-norm can be obtained in the next section. However, the modified two-grid algorithm is no longer parallel on the fine grid level.

4. Theoretical analysis

In this section, we shall analyze the stability and convergence of the modified two-grid method. It is clearly shown that this decoupling method is stable unconditionally and is of the same order of approximation accuracy as the coupling algorithm with a properly chosen coarse grid.

For convenience, we let C denote some positive constants and may stand for different values at its different occurrences.

4.1. Stability analysis

The following theorem provides the stability of the scheme (3.6)–(3.8).

Theorem 4.1. *Let $(\overline{u}^h, \overline{p}^h, \overline{\varphi}^h)$ be the solution of the problem (3.6)–(3.8), we have*

$$gk_{\min}\|\nabla\overline{\varphi}^h\|^2_{L^2(\Omega_p)} \le R_1^2 \tag{4.1}$$

$$\nu\|\nabla(\overline{u}^h)\|^2_{L^2(\Omega_f)} \le R_2^2, \tag{4.2}$$

$$\|\overline{p}^h\|_{L^2(\Omega_f)} \le R_3 \tag{4.3}$$

where

$$R_1 = \left(\frac{2g\widetilde{C}_p^2}{k_{\min}}\|f_2\|^2_{L^2(\Omega_p)} + \frac{2gC_t^2\widetilde{C}_t^2}{\nu k_{\min}}C_1\right)^{\frac{1}{2}},$$

$$R_2 = \left(\frac{2C_p^2}{\nu}\|f_1\|^2_{L^2(\Omega_f)} + \frac{2gC_t^2\widetilde{C}_t^2}{\nu k_{\min}}R_1^2\right)^{\frac{1}{2}},$$

$$R_3 = C_t\widetilde{C}_t\sqrt{\frac{g}{k_{\min}}}R_1 + \left(\sqrt{\nu} + 2C_t^2\alpha\sqrt{\frac{g}{k_{\min}}}\right)R_2 + C_p\|f_1\|_{L^2(\Omega_f)},$$

with

$$C_1 = \frac{C_p^2}{\nu}\|f_1\|^2_{L^2(\Omega_f)} + \frac{g\widetilde{C}_p^2}{k_{\min}}\|f_2\|^2_{L^2(\Omega_p)}.$$

Proof. First, taking $z_H = w_H$ in (3.4), $q_H = p_H$ in (3.5), and noting that

$$a_\Gamma(w_H, w_H) = 0 \quad \forall\, w_H \in W_H, \tag{4.4}$$

we can get

$$a_f(u_H, u_H) + a_p(\varphi_H, \varphi_H) = (f_1, u_H)_{\Omega_f} + g(f_2, \varphi_H)_{\Omega_p}. \tag{4.5}$$

By using the Hölder, Poincaré and Young inequalities, it follows that

$$\begin{aligned}\nu\|\nabla u_H\|^2_{L^2(\Omega_f)} + gk_{\min}\|\nabla\varphi_H\|^2_{L^2(\Omega_p)} &\le C_p\|f_1\|_{L^2(\Omega_f)}\|\nabla u_H\|_{L^2(\Omega_f)} + g\widetilde{C}_p\|f_2\|_{L^2(\Omega_p)}\|\nabla\varphi_H\|_{L^2(\Omega_p)} \\ &\le \frac{\nu}{2}\|\nabla u_H\|^2_{L^2(\Omega_f)} + \frac{gk_{\min}}{2}\|\nabla\varphi_H\|^2_{L^2(\Omega_p)} + \frac{C_p^2}{2\nu}\|f_1\|^2_{L^2(\Omega_f)} + \frac{g\widetilde{C}_p^2}{2k_{\min}}\|f_2\|^2_{L^2(\Omega_p)}.\end{aligned} \tag{4.6}$$

Consequently,

$$\nu\|\nabla u_H\|^2_{L^2(\Omega_f)} + gk_{\min}\|\nabla\varphi_H\|^2_{L^2(\Omega_p)} \le \frac{C_p^2}{\nu}\|f_1\|^2_{L^2(\Omega_f)} + \frac{g\widetilde{C}_p^2}{k_{\min}}\|f_2\|^2_{L^2(\Omega_p)}. \tag{4.7}$$

Then, letting $\psi_h = \overline{\varphi}^h$ in (3.6) gives

$$\begin{aligned}gk_{\min}\|\nabla\overline{\varphi}^h\|^2_{L^2(\Omega_p)} &\le g(f_2, \overline{\varphi}^h)_{\Omega_p} + g\int_\Gamma \overline{\varphi}^h u_H\cdot n_f\,ds \\ &\le g\widetilde{C}_p\|f_2\|_{L^2(\Omega_p)}\|\nabla\overline{\varphi}^h\|_{L^2(\Omega_p)} + gC_t\widetilde{C}_t\|\nabla\overline{\varphi}^h\|_{L^2(\Omega_p)}\|\nabla u_H\|_{L^2(\Omega_f)} \\ &\le \frac{gk_{\min}}{2}\|\nabla\overline{\varphi}^h\|^2_{L^2(\Omega_p)} + \frac{g\widetilde{C}_p^2}{k_{\min}}\|f_2\|^2_{L^2(\Omega_p)} + \frac{gC_t^2\widetilde{C}_t^2}{k_{\min}}\|\nabla u_H\|^2_{L^2(\Omega_f)}.\end{aligned} \tag{4.8}$$

We thus obtain (4.1) from (4.8) and (4.7).

In addition, by taking $v_h = \overline{u}^h$ in (3.7) and $q_h = \overline{p}^h$ in (3.8), we have

$$\begin{aligned}\nu\|\nabla\overline{u}^h\|^2_{L^2(\Omega_f)} &\le (f_1, \overline{u}^h)_{\Omega_f} - g\int_\Gamma \overline{\varphi}^h\overline{u}^h\cdot n_f\,ds \\ &\le C_p\|f_1\|_{L^2(\Omega_f)}\|\nabla\overline{u}^h\|_{L^2(\Omega_f)} + gC_t\widetilde{C}_t\|\nabla\overline{\varphi}^h\|_{L^2(\Omega_p)}\|\nabla\overline{u}^h\|_{L^2(\Omega_f)} \\ &\le \frac{\nu}{2}\|\nabla\overline{u}^h\|^2_{L^2(\Omega_f)} + \frac{C_p^2}{\nu}\|f_1\|^2_{L^2(\Omega_f)} + \frac{g^2C_t^2\widetilde{C}_t^2}{\nu}\|\nabla\overline{\varphi}^h\|^2_{L^2(\Omega_p)}.\end{aligned} \tag{4.9}$$

Hence,

$$\nu\|\nabla\overline{u}^h\|^2_{L^2(\Omega_f)} \le \frac{2C_p^2}{\nu}\|f_1\|^2_{L^2(\Omega_f)} + \frac{2g^2C_t^2\widetilde{C}_t^2}{\nu}\|\nabla\overline{\varphi}^h\|^2_{L^2(\Omega_p)}. \tag{4.10}$$

Combining (4.10) with (4.1) leads to (4.2).

Finally, to show (4.3), we consider the inf–sup condition (3.1) and (3.7),

$$\begin{aligned}\beta\|\overline{p}^h\|_{L^2(\Omega_f)} &\le \frac{(\nabla\cdot v_h, \overline{p}^h)}{\|\nabla v_h\|_{L^2(\Omega_f)}} \\ &\le \frac{\left|-a_f(\overline{u}^h, v_h) + (f_1, v_h)_{\Omega_f} - g\int_\Gamma \overline{\varphi}^h v_h\cdot n_f\,ds\right|}{\|\nabla v_h\|_{L^2(\Omega_f)}} \\ &\le \left(\nu + \alpha\sqrt{\frac{\nu g}{k_{\min}}}C_t^2\right)\|\nabla\overline{u}^h\|_{L^2(\Omega_f)} + C_p\|f_1\|_{L^2(\Omega_f)} + gC_t\widetilde{C}_t\|\nabla\overline{\varphi}^h\|_{L^2(\Omega_p)}.\end{aligned} \tag{4.11}$$

Then (4.3) follows from (4.1), (4.2) and (4.11). □

4.2. Convergence analysis

In this subsection, we consider the convergence of the modified two-grid method. Moreover, we assume the solution (u, p, φ) of (2.1)–(2.8) satisfies $u \in (H^2(\Omega_f))^d$, $p \in H^1(\Omega_f)$ and $\varphi \in H^2(\Omega_p)$.

The following lemma about the convergence of the coupling scheme can be found in [25].

Lemma 4.1. *For the problem (3.2)–(3.3), we have the following error estimate*

$$\|w - w_h\|_W + \|p - p_h\|_{L^2(\Omega_f)} \le Ch. \tag{4.12}$$

Then, we shall give the convergence of the modified two-grid algorithm (Algorithm 2).

Theorem 4.2. *Let $(\overline{u}^h, \overline{p}^h, \overline{\varphi}^h)$ be the solution to the problem (3.6)–(3.8), we have the following error estimates:*

$$\|\nabla(\varphi - \overline{\varphi}^h)\|_{L^2(\Omega_p)} \le C(h + H^2), \tag{4.13}$$

$$\|\nabla(u - \overline{u}^h)\|_{L^2(\Omega_f)} \le C(h + H^2), \tag{4.14}$$

$$\|p - \overline{p}^h\|_{L^2(\Omega_f)} \le C(h + H^2). \tag{4.15}$$

Proof. From [25], we have the error estimate:

$$\|\nabla(\varphi_h - \overline{\varphi}^h)\|_{L^2(\Omega_p)} \le CH^2. \tag{4.16}$$

Hence (4.13) can be at once obtained from (4.12) and (4.16).

In what follows, we shall prove (4.14) and (4.15).

Taking $z_h = (v_h, 0)$ in (3.2) and considering $b(z_h, p_h) = b_f(v_h, p_h)$, gives

$$a_f(u_h, v_h) + b_f(v_h, p_h) + g\int_\Gamma \varphi_h v_h \cdot n_f ds = (f_1, v_h)_{\Omega_f} \quad \forall v_h \in H_{fh} \tag{4.17}$$

$$b_f(u_h, q_h) = 0 \quad \forall q_h \in Q_h. \tag{4.18}$$

By comparing the problems (4.17)–(4.18) and (3.7)–(3.8), it follows that

$$a_f(u_h - \overline{u}^h, v_h) + b_f(v_h, p_h - \overline{p}^h) = -g\int_\Gamma (\varphi_h - \overline{\varphi}^h) v_h \cdot n_f ds \quad \forall v_h \in H_{fh} \tag{4.19}$$

$$b_f(u_h - \overline{u}^h, q_h) = 0 \quad \forall q_h \in Q_h. \tag{4.20}$$

Setting $v_h = u_h - \overline{u}^h$ in (4.19) and $q_h = p_h - \overline{p}^h$ in (4.20), we have

$$\begin{aligned} \nu\|\nabla(u_h - \overline{u}^h)\|^2_{L^2(\Omega_f)} &\le a_f(u_h - \overline{u}^h, u_h - \overline{u}^h) \\ &= -g\int_\Gamma (\varphi_h - \overline{\varphi}^h)(u_h - \overline{u}^h) \cdot n_f ds \\ &\le C_t\widetilde{C}_t g\|\nabla(\varphi_h - \overline{\varphi}^h)\|_{L^2(\Omega_p)}\|\nabla(u_h - \overline{u}^h)\|_{L^2(\Omega_f)}. \end{aligned} \tag{4.21}$$

Eliminating one $\|\nabla(u_h - \overline{u}^h)\|_{L^2(\Omega_f)}$ on both sides of (4.21) and applying (4.16), we can deduce that

$$\|\nabla(u_h - \overline{u}^h)\|_{L^2(\Omega_f)} \le CH^2. \tag{4.22}$$

Next, in view of (4.19) and inf–sup condition (3.1), we arrive at

$$\begin{aligned} \beta\|p_h - \overline{p}^h\|_{L^2(\Omega_f)} &\le \frac{b(v_h, p_h - \overline{p}^h)}{\|\nabla v_h\|_{L^2(\Omega_f)}} \\ &\le \frac{|a_f(u_h - \overline{u}^h, v_h)| + \left|g\int_\Gamma (\varphi_h - \overline{\varphi}^h) v_h \cdot n_f ds\right|}{\|\nabla v_h\|_{L^2(\Omega_f)}} \\ &\le C(\|\nabla(u_h - \overline{u}^h)\|_{L^2(\Omega_f)} + \|\nabla(\varphi_h - \overline{\varphi}^h)\|_{L^2(\Omega_p)}). \end{aligned} \tag{4.23}$$

Using (4.22) and (4.16), yields

$$\|\nabla(p_h - \overline{p}^h)\|_{L^2(\Omega_f)} \le CH^2. \tag{4.24}$$

Applying triangle inequalities and (4.12) to (4.22) and (4.24), then (4.14) and (4.15) follow. □

By comparing the contents of Lemma 4.1 and Theorem 4.2, we can observe that the approximate solution $(\overline{u}^h, \overline{p}^h, \overline{\varphi}^h)$ produced by the modified two-grid method is as accurate as the approximation produced by the coupling method when we choose $h = H^2$, which can be shown by the numerical experiments in the next section.

Table 1
The convergence performance and CPU time of the coupling scheme.

h	$\Vert\nabla e_h^{\varphi}\Vert_{L^2(\Omega_m)}$	Rate	$\Vert\nabla e_h^{u}\Vert_{L^2(\Omega_c)}$	Rate	$\Vert e_h^{p}\Vert_{L^2(\Omega_c)}$	Rate	CPU
$\frac{1}{4}$	1.55688	–	1.88956	–	1.49885	–	0.027
$\frac{1}{16}$	0.36783	1.04076	0.36779	1.18054	0.15109	1.65519	1.835
$\frac{1}{64}$	0.09258	0.99510	0.091039	1.00717	0.03573	1.03996	220.259

Table 2
The convergence performance and CPU time of the modified two-grid scheme.

h	$\Vert\nabla e_h^{\overline{\varphi}}\Vert_{L^2(\Omega_m)}$	Rate	$\Vert\nabla e_h^{\overline{u}}\Vert_{L^2(\Omega_c)}$	Rate	$\Vert e_h^{\overline{p}}\Vert_{L^2(\Omega_c)}$	Rate	CPU
$\frac{1}{4}$	1.57518	–	1.52308	–	1.35077	–	0.014
$\frac{1}{16}$	0.38733	1.01194	0.36562	1.02928	0.14881	1.59111	0.151
$\frac{1}{64}$	0.09482	1.01508	0.08957	1.01456	0.02989	1.15779	2.373

5. Numerical experiments

In this section, we shall first give a numerical experiment to demonstrate the effectiveness of the modified two-grid method by comparing the numerical results of the coupling scheme and the modified two-grid scheme and their computational time. Then we consider another experiment to examine the effects of the hydraulic conductivity tensor **K**.

We assume that the computational domain $\Omega_f = (0, 1) \times (1, 2)$ and $\Omega_p = (0, 1) \times (0, 1)$ with interface $\Gamma = (0, 1) \times \{1\}$. The finite element spaces we used are the well-known Mini elements ($P1b$—$P1$) for the Stokes fluid and the linear Lagrangian elements ($P1$) for the Darcy flow. And the relation between the coarse mesh size H and the fine mesh size h is chosen as $h = H^2$. Moreover, we apply the software package FreeFEM++ to implement the algorithms and all results are generated by the same computer.

For simplicity of notation, we denote

$$e_h^{\vartheta} = \vartheta_h - \vartheta, \qquad e_h^{\overline{\vartheta}} = \overline{\vartheta}^h - \vartheta,$$

where ϑ can be φ, u, p.

Experiment 1. We set the physical parameters g, ν, α equal to 1, $\mathbf{K} = \mathbf{I}$, and the exact solution is

$$\begin{cases} u = \left([x^2(y-1)^2 + y], \left[-\frac{2}{3}x(y-1)^3 + 2 - \pi \sin(\pi x)\right]\right), \\ p = [2 - \pi \sin(\pi x)] \sin\left(\frac{\pi}{2}y\right), \\ \phi = [2 - \pi \sin(\pi x)][1 - y - \cos(\pi y)]. \end{cases}$$

The forcing terms and the boundary conditions follow the exact solution.

In Table 1, we list the errors between the exact solution and the finite element approximate solutions of the coupled problem, convergent rates and computational time with the mesh size $h = 1/4, 1/16, 1/64$. We can observe that the errors for $\nabla\varphi$, ∇u and p in the L^2-norm are all around the order of $O(h)$.

In Table 2, we show the convergence performance and computational time of the modified two-grid scheme. Apparently, the order of convergence is all of $O(h)$, especially that of p in L^2-norm is much better than expected. Consequently, numerical experiments verify the theoretical results in (4.13)–(4.15). In addition, we note that the CPU time used by the modified two-grid scheme is much less than that of the coupling scheme. Thus we conclude that the modified two-grid scheme is effective.

Experiment 2. We take $\mathbf{K} = K\mathbf{I}$ and choose the exact solution is

$$\begin{cases} u = (y^2 - 2y + 1, x^2 - x), \\ p = 2(x + y - 1) + \frac{g}{3K}, \\ \varphi = \frac{1}{K}\left[x(1-x)(y-1) + \frac{1}{3}y^3 - y^2 + y\right] + \frac{2}{g}x. \end{cases}$$

The boundary conditions and forcing terms follow the exact solution, the physical parameters g, ν, and α are the same as in Definition 1.

In Tables 3–5, we list the convergence performance of the modified two-grid scheme with $\mathbf{K} = \mathbf{I}$, $0.1\mathbf{I}$, $0.01\mathbf{I}$, respectively. Observe that, the errors of $\nabla\varphi$, ∇u and p in L^2-norm increase as K decreases, especially of $\nabla\varphi$, while the convergence rates go to 1 when h goes to 0, even though the rates may be much larger or smaller than 1 when h is not small enough.

Table 3
The convergence performance and CPU time of the modified two-grid scheme with $\mathbf{K} = \mathbf{I}$.

h	$\|\nabla e_h^{\overline{\varphi}}\|_{L^2(\Omega_m)}$	Rate	$\|\nabla e_h^{\overline{u}}\|_{L^2(\Omega_c)}$	Rate	$\|e_h^{\overline{p}}\|_{L^2(\Omega_c)}$	Rate	CPU
$\frac{1}{4}$	0.15585	–	0.21702	–	0.17477	–	0.012
$\frac{1}{16}$	0.03631	1.05086	0.04645	1.11195	0.02296	1.46392	0.127
$\frac{1}{64}$	0.00891	1.01319	0.01115	1.02930	0.00371	1.31371	2.082

Table 4
The convergence performance and CPU time of the modified two-grid scheme with $\mathbf{K} = 0.1\mathbf{I}$.

h	$\|\nabla e_h^{\overline{\varphi}}\|_{L^2(\Omega_m)}$	Rate	$\|\nabla e_h^{\overline{u}}\|_{L^2(\Omega_c)}$	Rate	$\|e_h^{\overline{p}}\|_{L^2(\Omega_c)}$	Rate	CPU
$\frac{1}{4}$	1.55857	–	0.21704	–	0.24255	–	0.012
$\frac{1}{16}$	0.36363	1.04980	0.04649	1.11139	0.04346	1.24012	0.127
$\frac{1}{64}$	0.08959	1.01050	0.01117	1.02874	0.01096	0.99364	2.082

Table 5
The convergence performance and CPU time of the modified two-grid scheme with $\mathbf{K} = 0.01\mathbf{I}$.

h	$\|\nabla e_h^{\overline{\varphi}}\|_{L^2(\Omega_m)}$	Rate	$\|\nabla e_h^{\overline{u}}\|_{L^2(\Omega_c)}$	Rate	$\|e_h^{\overline{p}}\|_{L^2(\Omega_c)}$	Rate	CPU
$\frac{1}{4}$	15.58570	–	0.21906	–	1.48650	–	0.012
$\frac{1}{16}$	3.76241	1.02525	0.05896	0.94669	0.69558	0.54780	0.127
$\frac{1}{64}$	0.93566	1.00379	0.01519	0.97826	0.19101	0.93228	2.083

6. Conclusions

In a word, we proposed a modified two-grid algorithm for the mixed Stokes–Darcy problem. Unconditional stability is proved, and the optimal error estimates are obtained. To demonstrate the effectiveness of the modified two-grid algorithm we conduct the numerical experiments, which confirm the theoretic estimates.

References

[1] Y. Boubendir, S. Tlupova, Domain decomposition methods for solving Stokes–Darcy problems with boundary integrals, SIAM J. Sci. Comput. 35 (2013) B82–B106.
[2] Y.Z. Cao, M. Gunzburger, X.M. He, X.M. Wang, Robin-Robin domain decomposition methods for the steady-state Stokes–Darcy system with the Beavers–Joseph interface condition, Numer. Math. 117 (2011) 601–629.
[3] Y.Z. Cao, M. Gunzburger, X.M. He, X.M. Wang, Parallel, non-iterative, multi-physics domain decomposition methods for time-dependent Stokes–Darcy systems, Math. Comp. 83 (2014) 1617–1644.
[4] W. Chen, M. Gunzburger, F. Hua, X.M. Wang, A parallel robin–robin domain decomposition method for the Stokes–Darcy system, SIAM J. Numer. Anal. 49 (2011) 1064–1084.
[5] M. Discacciati, Domain decomposition methods for the coupling of surface and groundwater flows Ph.D. dissertation, École Polytechnique Fédérale de Lausanne, 2004.
[6] M. Discacciati, E. Miglio, A. Quarteroni, Mathematical and numerical models for coupling surface and groundwater flows, Appl. Numer. Math. 43 (2002) 57–74.
[7] M. Discacciati, A. Quarteroni, Convergence analysis of a subdomain iterative method for the finite element approximation of the coupling of Stokes and Darcy equations, Comput. Vis. Sci. 6 (2004) 93–103.
[8] M. Discaaaiati, A. Quarteroni, A. Valli, Robin–Robin domain decomposition methods for the Stokes–Darcy coupling, SIAM J. Numer. Anal. 45 (2007) 1246–1268.
[9] M. Discacciati, A. Quarteroni, Analysis of a domain decomposition method for the coupling Stokes and Darcy equations, in: F. Brezzi, et al. (Eds.), Numerical Analysis and Advanced Applications—Enumath 2001, Springer, Milan, 2003, pp. 3–20.
[10] W.Q. Feng, X.M. He, Z. Wang, X. Zhang, Non-iterative domain decomposition methods for a non-stationary Stokes–Darcy model with the Beavers–Joseph interface condition, Appl. Math. Comput. 219 (2012) 453–463.
[11] J. Galvis, M. Sarkis, Balancing domain decomposition methods for mortar coupling Stokes–Darcy Systems, in: Proceedings of the 16th International Conference on Domain Decomposition Methods, 2005.
[12] B. Jiang, A parallel domain decomposition method for coupling of surface and groundwater flows, Comput. Methods Appl. Mech. Engrg. 198 (2009) 947–957.
[13] R. Glowinski, T. Pan, J. Periaux, A Lagrange multiplier/fictitious domain method for the numerical simulation of incompressible viscous flow around moving grid bodies: I. Case where the rigid body motions are known a priori, C. R. Acad. Sci. Paris Sér. I Math. 324 (1997) 361–369.
[14] W.J. Layton, F. Schieweck, I. Yotov, Coupling fluid flow with porous media flow, SIAM J. Numer. Anal. 40 (2003) 2195–2218.
[15] S. Markus, E. Houstis, A. Catlin, J. Rice, P. Tsompanopoulou, E. Vavalis, D. Gottfried, K. Su, G. Balakrishnan, An agent-based netcentric framework for multidisciplinary problem solving environments (MPSE), Int. J. Comput. Eng. Sci. 1 (2000) 33–60.
[16] M. Mu, Solving composite problems with interface relaxation, SIAM J. Sci. Comput. 20 (1999) 1394–1416.
[17] M.C. Cai, M. Mu, J.C. Xu, Preconditioning techniques for a mixed Stokes/Darcy model in porous media applications, J. Comput. Appl. Math. 233 (2009) 346–355.
[18] A. Marquez, S. Meddahi, F.J. Sayas, A decoupled preconditioning technique for a mixed Stokes–Darcy model, J. Sci. Comput. 57 (2013) 174–192.
[19] M. Mu, X.H. Zhu, Decoupled schemes for a non-stationary mixed Stokes–Darcy model, Math. Comp. 79 (2010) 707–731.
[20] M. Kubacki, Uncoupling evolutionary groundwater–surface water flows using Crank–Nicolson LeapFrog method, Numer. Methods Partial Differential Equations 29 (2013) 1192–1216.
[21] L. Shan, H.B. Zheng, Partitioned time stepping method for fully evolutionary Stokes–Darcy flow with the Beavers–Joseph interface conditions, SIAM J. Numer. Anal. 51 (2013) 813–839.

[22] L. Shan, H.B. Zheng, W.J. Layton, A decoupling method with different subdomain time steps for the nonstationary Stokes–Darcy model, Numer. Methods Partial Differential Equations 29 (2013) 549–583.
[23] M.C. Cai, M. Mu, J.C. Xu, Numerical solution to a mixed Navier–Stokes/Darcy model by the two-grid approach, SIAM J. Numer. Anal. 47 (2009) 3325–3338.
[24] P. Chtdyagwai, B. Rivière, A two-grid method for coupled free flow with porous media flow, Adv. Water Resour. 34 (2011) 1113–1123.
[25] M. Mu, J.C. Xu, A two-grid method of a mixed Stokes–Darcy model for coupling fluid flow with porous media flow, SIAM J. Numer. Anal. 45 (2007) 1801–1813.
[26] M.C. Cai, M. Mu, A multilevel decoupled method for a mixed Stokes/Darcy model, J. Comput. Appl. Math. 236 (2012) 2452–2465.